MAPPING THE EFFECTS OF KNOTS ON LOBLOLLY PINE LUMBER

by

STEPHEN LOUIS WRIGHT JR.

(Under the Direction of Joseph Dahlen and Cristian Montes)

ABSTRACT

Loblolly pine (*Pinus taeda*) plantation rotation lengths have decreased due to the implementation of intensive forest management. Lumber extracted from younger plantations will tend to have lower stiffness (modulus of elasticity (MOE)) and strength (modulus of rupture (MOR)) than lumber from older plantations. This study analyzed the knots of dimension lumber sourced from intensively managed 24 to 33-year-old trees harvested from the Lower Coastal Plain in Georgia. The aim of the research was to develop a rapid method to evaluate knots and develop models that predict lumber stiffness and strength. The methodology involved image evaluation using a semi-automated process using K-means clustering to identify the knots from the clearwood. For each piece of lumber, a rectangle was overlaid on to each knot with the summed rectangle areas divided by the total surface area of the lumber to calculate the knot area ratio (KAR). Lumber stiffness was best modeled using KAR and specific gravity; the linear model had a R^2 of 0.69 with RMSE of 1.29 GPa. The variation in lumber strength was best described by KAR and MOE_{dyn} which yielded a R^2 of 0.53 with a RMSE of 8.47 MPa. Significant differences were found in MOR when lumber was classified into three failure type categories: in clearwood (43.8 MPa), at a single knot (37.1 MPa), and at a combination of knots (32.4 MPa).

INDEX WORDS: branches, design values, image analysis, modulus of elasticity, modulus of rupture, wood quality.

MAPPING THE EFFECTS OF KNOTS ON LOBLOLLY PINE LUMBER

by

STEPHEN LOUIS WRIGHT JR.

B.S., University of Georgia, 2015

A Thesis Submitted to the Graduate Faculty of The University of Georgia in Partial Fulfillment

of the Requirements for the Degree

MASTER OF SCIENCE

ATHENS, GEORGIA

2017

© 2017

Stephen Louis Wright Jr.

All Rights Reserved

MAPPING THE EFFECTS OF KNOTS ON LOBLOLLY PINE LUMBER

by

STEPHEN LOUIS WRIGHT JR.

Major Professors: Joseph Dahlen
Cristian Montes

Committee: Pete Bettinger
Lawrence Morris

Electronic Version Approved:

Suzanne Barbour
Dean of the Graduate School
The University of Georgia
December 2017

TABLE OF CONTENTS

CHAPTER 1: INTRODUCTION ... 1
Purpose of study ... 1
How the study is original ... 1
CHAPTER 2: LITERATURE REVIEW ... 3
History and importance of loblolly pine ... 3
Southern Silvicultural Practices ... 3
Wood quality factors ... 7
Nondestructive testing of lumber quality ... 9
Lumber grading and the Southern Pine Inspection Bureau ... 10
Image analysis ... 11
Knot detection ... 12
References ... 16
CHAPTER 3: MAPPING THE EFFECTS OF KNOTS ON LOBLOLLY PINE LUMBER ... 22
Abstract ... 23
1 Introduction ... 24
2 Materials and methods ... 27
3 Results and discussion ... 35
Conclusions ... 43
References ... 45
CHAPTER 4: CONCLUSIONS ... 48

LIST OF TABLES

Table 3.1 Allowable knot sizes by lumber size and number for visually graded lumber. 25
Table 3.2 Summary statistics for the variables used in model development. 36
Table 3.3 Pearson correlation matrix among lumber properties used to model stiffness and strength. 37
Table 3.4 Model performance for prediction of lumber stiffness and strength using KAR_{actual} and $KAR_{rectangle}$. 38
Table 3.5 Prediction of modulus of elasticity using KAR and nondestructive lumber characteristics. 39
Table 3.6 Prediction of MOR using KAR_{actual} and nondestructive lumber characteristics........... 40
Table 3.7 Modulus of elasticity, modulus of rupture, $KAR_{rectangle}$, specific gravity and acoustic velocity values based on type of failure. Significant differences between the types of failure (α=0.05) indicated by letters.. 42
Table 3.8 Shows the breakdown of type of lumber failure based on lumber size. 43

LIST OF FIGURES

Fig. 3.1 The image analysis workflow performed on each piece of lumber containing knots. 30
Fig. 3.2 Example of image processing and analysis method of lumber. Image (A) is the rough cropped image. Image (B) is the rough cropped image with a white mask applied. Image (C) shows the lumber with the initial knot detection, and image (D) shows an image with the distortion removed. 31
Fig. 3.3 (A) refers to KAR_{actual} where only the black area is considered and (B) refers $KAR_{rectangle}$ where the whole area encompassed in the dotted rectangle. 32
Fig. 3.4 The inverse relationship between square root $KAR_{rectangle}$ and modulus of elasticity and modulus of rupture.. 38
Fig. 3.5 Relationship between lumber stiffness, rectangle knot area ratio, and dynamic MOE with the regression pane from best model. 39
Fig. 3.6 Relationship between lumber strength, rectangle knot area ratio, and dynamic MOE with the regression pane from best model. 40
Fig. 3.7 Example of a 2 × 6 with the location of failure in clearwood. 41
Fig. 3.8 Example of a 2 × 6 with the location of failure at a knot. 41
Fig. 3.9 Example of a 2 × 6 with the location of failure in at combination knots. 41

CHAPTER 1: INTRODUCTION

Purpose of study

Four major pine species, loblolly pine (*Pinus taeda*), longleaf pine (*Pinus palustris*), shortleaf pine (*Pinus enchinata*) and slash pine (*Pinus elliotii*), are intensively managed in the Southeastern United States. Of these species, loblolly pine is the most widely planted and commercially important (McKeand et al. 2003). Improved silvicultural practices and genetics have enabled loblolly pine trees to grow to chip-n-saw and sawtimber merchantability in shorter rotation lengths (Amateis 2000; Munsell and Fox 2010). However, these fast growing trees have been linked to lower mechanical properties because of their much larger volume of corewood (Cramer et al. 2005). Lumber sourced from intensively managed stands have been shown to have decreased stiffness and strength properties (Roth et al. 2007). This research provides a framework for future work to cost-effectively evaluate knots in a laboratory setting. By evaluating knots, important factors such as lumber strength and stiffness can be better predicted.

How the study is original

The present study analyzed images of loblolly pine (*Pinus taeda*) dimension lumber sourced from intensively managed trees ages 24-33 in the Lower Coastal Plain of Georgia. Knots were identified using a classification algorithm (K-means clustering). . The classification algorithm provided the locations (x,y) and absolute area of every knot. Two different methods of knot summations were developed. Actual knot area ratio (KAR_{actual}) was calculated by summing the areas of all the knots and dividing by the surface area of the lumber. Rectangle knot area ratio ($KAR_{rectangle}$) was calculated by overlaying a rectangle on to each knot and counting all the area within the rectangle as knotty wood. The sums of the rectangles were then divided by the surface area of the lumber. The results of this study suggest that image analysis is an effective way to measure knot information of lumber.

CHAPTER 2: LITERATURE REVIEW

History and importance of loblolly pine

Prior to European settlement of the Southeastern United States, loblolly pine (*Pinus taeda)* was a relatively small component in the forested landscape. The uplands were dominated by longleaf pines (*Pinus palustris*) and mixed hardwoods such as white oak (*Quercus alba*), red oak (*Quercus rubra*) and tulip poplar (*Liriodendron tulipifera*), while the bottomlands consisted of bald cypress (*Taxodium distichum*) and black tupelo (*Nyssa sylvatica*) (Schultz 1999). Following European arrival, most of the old-growth forests were cleared for timber and space to conduct extensive row-crop agriculture (Carter et al. 2015). Soil erosion and nutrient depletion due to poor farming practices coupled with low commodity prices, led to an abundance of abandoned agricultural land in the 1950's (Schultz 1999; Pfeffer et al. 2006). With its ability to grow well across a variety of eroded sites, loblolly pine trees were planted on the abandoned farmland (Schultz 1997). By the mid-20th century there was approximately 81,000 hectares of planted pines across the Southeast and by the end of the century there were over 12 million hectares (Wear and Greis 2002). The rapid growth in response to silvicultural treatments coupled with market value of pulpwood and sawtimber has made loblolly pine the most important southern pine (Borders and Bailey 2001; Rausher and Johnsen 2004; Mei and Clutter 2014).

Southern Silvicultural Practices

Initial planting density

Determining desired forest products prior to stand establishment is one of the most important keys to creating an economically successful stand (Bailey 1986). If the desired product is pulpwood, it may be better to plant at a higher initial density because wood quality and individual tree form are not usually of concern. More densely planted stands tend to have smaller diameter branches and boles. If the desired product is sawtimber, the initial density might be lower to help facilitate diameter growth, decrease self-thinning and sustain good tree form (Amateis and Burkhart 2012). However, less dense stands in conjunction with more intensive management regimes have been linked to larger branch size and branch angle, especially in the first log (Borders and Volfovicz 2012).

Tree improvement

Through decades of development and proven financial returns, genetically improved trees via selection have become a mainstay of intensive forest management (IFM) practices (Fox et al. 2007b). Compared to unimproved loblolly pine stand volume, open-pollinated first-generation trees have 7% to 12% greater stand volume, with 13% to 21% greater volume for second generation (Li et al. 1999). Martin and Shiver (2002) found similar results with first generation trees increasing total volume up to 16% in the Coastal Plain and up to 19% in the Piedmont. Further, McKeand et al. (2003) determined that full-sibs and clonal trees can increase stand yield by 35% and 50% compared to unimproved trees. In addition to growth, disease resistance, bole straightness, branch angle, forking and ramicorn branches are under very strong genetic control (Isik et al. 2005; Sorensson 2006; Xiong et al. 2014; Weng et al. 2017).

Competing vegetation control

Competing vegetation control, which reduces unwanted woody and herbaceous vegetation, is common in intensively managed pine plantations. It is often carried out by applying a mixture of herbicides via broadcast or banded spraying (Jokela et al. 2010). Siry (2002) estimated that nearly 800,000 hectares receive some form of herbicide control in the southeastern United States on a yearly basis. Competition control has shown to produce strong gains in total volume, merchantable volume and diameter increase because it increases growing space and nutrient availability (Martin and Shiver 2002). Herbaceous control was shown to increase productivity of loblolly pine between 9 and 18 m^3 ha^{-1} per year in located across the Southeast (Fortson et al. 1996). Martin and Shiver (2002) found that that total volume gains of 39% to 45% can be expected from complete vegetation control in loblolly plantations in the Southeastern Piedmont and Lower Coastal Plain.

Fertilization

As with initial planting density and competing vegetation control, fertilization is also an important management tool used to increase plantation productivity (Jokela and Long 2000). Fertilizer increases the size of individual needle follicles thus increasing light interception area which in turn increases photosynthesis (Shultz 1997). Fox et al. (2007a) performed a marginal analysis illustrating typical financial returns following nitrogen and phosphorous application. Using average prices for urea and diammonium phosphate, it would roughly cost $37 to fertilize a hectare of forest. A hectare of fertilized forest showed an increased revenue of $157 with an internal rate of return of 19%. Herbicide and fertilization of loblolly stands in southwest Georgia showed that by age 15, total stand volume had increased by 62% percent versus the control stands (Gräns et al. 2016). Fertilization has become increasingly popular tool with roughly

26,000 hectares fertilized yearly and 6.5 million hectares being fertilized between 1969 and 2004 (Siry 2002; Albaugh et al. 2007).

Competition control & fertilization

In operational forestry, applying competition control and fertilization treatments are often not mutually exclusive. Borders et al. (2004) studied the effects of annual herbicide and fertilization applications in the Georgia Lower Coastal Plain. They found that at age 15, plots with the combined treatments had 44% more total biomass than the control. Jokela et al. (2000) examined 5 and 8-year growth rates and interactions between fertilization and competition control. At both Year 5 and Year 8, combination treatment plots ranged from 52% to 100% volume response to the fertilization and competition control treatments. The differences in volume response was attributed to different soil types between the plots. Jokela et al. (2000) suggested that the combination of treatments might be additive.

Thinning

Forest thinning consists of increasing growing space for desirable dominant crop trees by removing diseased or low values trees (Chase et al. 2016; Coble and Grogan 2016). When stands are established at higher stockings, there is intraspecific competition for fixed local resources which can lead to high stand mortality through self-thinning (Hennessey et al. 2004). The first commercial thinning is usually employed between ages of 13 to 15 with most of the merchantable product being pulpwood. The second commercial thinning is usually conducted during years 18-21 with additional pulpwood and some chip-n-saw being harvested. First and second thinnings are often conducted to provide mid-rotation cash flow, increase residual growing space and remove undesirable competition (Amateis 2000). A study by Sword Sayer et al. (2004) in the Western Gulf showed that the growth response by thinning alone accounted for nearly half the trees being chip-n-saw size by age 17, with plots that combined thinning and fertilization increasing the total number of trees to be in the chip-n-saw size by 70% compared to the control.

Wood quality factors

Wood quality

Wood quality is difficult to define because of the wide array of factors that need to be considered. Larson (1969) defines it as an idea that has been formulated to generalize the type, physical structure, chemical composition and shape of wood elements. Generally, wood quality depends on the intended end-use product (Gartner 2005). For example, the primary properties of importance for dimension lumber are stiffness and strength, warp and treatability (Gartner 2005). Factors that affect lumber stiffness and strength include the size and frequency of knots, density, slope of grain and microfibril angle (MFA). Conversely, if the desired product is pulp and paper, properties such as pulp yield and tracheid dimensions, which relate to paper smoothness and strength measures are of high importance (Gartner 2005).

Specific gravity

Specific gravity (SG) is a unitless metric of the density of wood relative to the density of water (Williamson and Wiemann 2010). It is a good predictor of pulp yield, lumber stiffness and strength (Smook 2002; Antony et al. 2010; Williamson and Wiemann 2010). In conifers, specific gravity is a function of the ratio between the earlywood (EW) and latewood (LW) of the cells and the specific gravity of each cell type. Earlywood cells are formed at the beginning of the yearly growth increment and latewood is formed during the latter portion (Cramer et al. 2005). Earlywood consists of wide cells with large lumens and thin cell walls, causing it to have lower strength properties when compared to LW cells, which have small lumens and thick cell walls (Cramer et al. 2005; Eberhardt and Samuelson 2015). The formation of the wider cells in EW has been attributed to the abundance of moisture available in the soil while LW can start forming during the onset of drought, however prolonged water deficits have been shown to decrease the length of LW formation periods (Kozlowski et al. 1991)

Clark et al. (2008) studied the effects of initial planting densities on specific gravity (SG) at age 21. They determined that the wider spaced trees had the lowest SG with the values being between 12 to 14% lower. They attributed the difference in SG is mostly attributed to the fact that the wider spaced trees had more natural resources (light, nutrients and water) and space to respond to management activities such as fertilization. In the same study, it was also found that SG decreased up the stem for the range of studied initial planting densities between 1.83 m by 2.44 m to 3.66 m by 3.66 m. The negative relationship between increased tree growth and SG was largely due to increased corewood resulting from the rapid growth in first 10 years post-stand establishment (Faust et al. 1999; Clark et al. 2005; Cramer et al. 2005). Faust et al. (1999) conducted image analysis of 2.5 cm thick cross section disks and showed that competition control decreases LW percent. Cramer et al. (2005) measured SG, microfibril angle and the presence of compression wood in earlywood and latewood and found that microfibril angle and SG could explain 75% of the variability in the modulus of elasticity for latewood but accounted for less than half the variability for earlywood. Specific gravity also varies by physiographic region with the Southern Atlantic Coastal and Gulf Coastal plains having higher values while Upper Coastal, Hilly Coastal and northern Atlantic plains and the Piedmont all had lower values (Clark and Saucier 1989; Jordan et al. 2008; Antony et al. 2010).

Microfibril angle

Microfibril angle (MFA) is the angle of the S_2 layer in the secondary cell walls of xylem cells (Donaldson 2008). The S_2 layer is the most important determinant of mechanical properties as it is the thickest of the three secondary layers (Abe and Funada 2005). Generally, the MFA of softwoods decreases with increasing distance from pith, tree height and age (Barnett and Bonham 2004; Jordan et al. 2007). Therefore, lumber sawn from fast growing intensively managed logs tend to have higher MFA. Like SG, MFA has been shown to be higher in the North Atlantic and Piedmont physiographic regions than the South Atlantic, Gulf Coastal and Hilly Coastal regions (Jordan et al. 2006; Jordan et al. 2007).

Corewood/outerwood & juvenile wood/mature wood

Corewood is defined for loblolly and radiata pine (*Pinus radiata*) as the zone of wood from the first growth ring from the pith to roughly the 15th ring, while outerwood is characterized as the rings formed after corewood production has stopped (Burdon et al. 2004). Corewood is the wood with widely spaced rings with high ring curvature, and outerwood is the wood with thinly spaced growth rings with low curvature (Burdon et al. 2004). Corewood is less desirable for solid wood products because it is less stiff, has lower SG, higher MFA, and greater tendency to warping, cupping and checking (Burdon et al. 2004; Lasserre et al. 2004; Davies et al. 2016). Generally, the largest determinant of amount of CW versus OW is tree age; however, silvicultural treatments such as fertilization and thinning also affect corewood to outerwood ratios (Lasserre et al. 2004: Raymond et al. 2008).

Nondestructive testing of lumber quality

Non-destructive evaluation methods of wood quality have been developing since the 1960's as a means of improving log sorting, wood utilization and lumber strength and stiffness prediction (Ross et al. 1991). Major methods of non-destructive evaluation include the evaluation of visual characteristics measured via sensors, physical tests such as electrical and vibrational properties, chemical tests, and mechanical tests such as proof loading (Ross 2015). Generally, non-destructive evaluation has been shown to effectively aid in the sorting of logs and lumber based on stiffness (Carter et al. 2006).

One of the most researched NDE method is using acoustic velocity to evaluate the stiffness of trees, logs, and lumber (Grabianowski et al. 2006; Mora et al. 2009; Chan et al. 2011; Lenz et al. 2013; Butler et al. 2017). Reasons for the use of acoustic velocity include its relative ease of data acquisition and generally positive research results (Carter et al. 2006; Wang et al. 2007). The relationship between dynamic MOE and acoustic velocity can be described by:

$$Dynamic\ MOE = \frac{AV^2 * density}{1{,}000{,}000{,}000} \quad (1)$$

where AV is acoustic velocity in meters/second, density in kg/m^3, and dynamic MOE in GPa. A moderate relationship between static MOE measured on small clear samples and standing tree dynamic MOE of loblolly pine was found by Mora et al. (2009) with $R^2 = 0.65$. Vikram et al. (2011) found a phenotypic correlation of 0.42 for small clear static MOE and log dynamic MOE of Douglas-fir.

Lumber grading and the Southern Pine Inspection Bureau

The lumber industry has developed methods for separating lumber into different strength categories based on visual analysis or non-destructive evaluation of lumber defects. Common defects evaluated include knots, pitch and wane (ASTM International 2006). Visual grading is completed by trained mill employees that examine the lumber for the size and nature of knots and other defects and grade it based on empirical rules developed by lumber grading associations (Schajer 2001; ASTM International 2006). The main lumber grading association in the U.S. South for southern pine lumber is the Southern Pine Inspection Bureau (SPIB). Visual lumber grading is prominently implemented at lower-production softwood sawmills and hardwood sawmills (Erikson et al. 2000). At high production softwood sawmills, visual machine grading is the norm (Galligan and McDonald 2000). Machine grading uses cameras and sensors that detect surface defects of each piece of lumber linked to computer control (Lycken 2006).

Image analysis

Image analysis is the process of obtaining numerical data from images and is becoming a popular method of data collection because it is non-invasive, quick and relatively low-cost to implement (Prats-Montalbán et al. 2011). An image is an array of pixels with each pixel containing a coordinate (x,y) pair with the x value indicating the distance from the left edge of the image and the y value indicating the distance from the top of the image. Each pixel in a red, green and blue (RGB) scale image has three layers with each layer corresponding to a single-color band. This allows for each layer to represent a segment of the electromagnetic spectrum. Each of the three layers is encoded as a number in a range between 0 and 255, with 0 representing darkness and 255 representing brightness (Russ and Russ 2007).

One method of image analysis is K-means clustering. K-means clustering is the minimizing of the mean squared distance from each data point to each *k* center with the number of *k* centers being defined by the user (Kanungo et al. 2002). This method of clustering has been widely deployed in a variety of scientific fields because of ease of implementation and computation speed (Jain 2010). Even though this method has been successfully implemented in many areas, it relies on the initial starting conditions (i.e. number of initial *k* centers) and the difficulty in determining these optimal starting conditions (Jain and Dubes 1988; Kanungo et al. 2002; Likas et al. 2003).

Knot detection

Roblot et al. (2010) utilized a system using E-Scan machine manufactured by LuxScan Technologies (Ehlerange, Luxembourg) to automatically detect knots from each face of dimension lumber milled from Douglas-fir (*Pseudotsuga menziesii*) and Norway spruce (*Picea excelsa*) logs. The automatic detection of the knots allowed for the computation of the knot area ratio (KAR). KAR is defined as the cross-sectional area of the knots divided by the total lumber cross section area. They analyzed 451 specimens, with 299 of the specimens containing pith and 152 without pith. Their objective was to determine if the algorithm could correctly match the knots on the different faces of the lumber with emphasis on the pieces containing the pith. A model was developed to predict MOR from KAR. The adjusted R^2 for the Douglas-fir model was between 0.59 and 0.72 with the R^2 for the Norway spruce was between 0.42 and 0.5. The range of R^2 is based on if the models used one, two or three explanatory parameters. The study showed that the determination of KAR coupled with MOE_{dyn} can provide accurate estimation of MOR.

Todoroki et al. (2010) designed a system to detect knots from images of Douglas-fir veneer sheets. In an effort to identify the location and size of knots. The images were sourced from a single tree that produced 51 full veneer sheet and 3 half sheets. High resolution images were captured of both faces of the veneer sheets, and then converted to grayscale and red component images prior to analysis. A two-phased algorithm was used in the image analysis to increase accuracy by decreasing the false detection of knots. The first phase applied a global approach (i.e. considered whole veneer sheet) and converted the images to grayscale and red components. This phase also segmented the regions of the sheets that demonstrated the potential to contain knots. The second phase applied a local approach (i.e. considered segments of the sheet) and applied adaptive thresholding to increase the accuracy of knot detection. The results of this study showed that the two-phased algorithm could accurately detect the size and location of knots in the images of veneer sheets. The red component images performed better than the grayscale images, with 78% of the knots being correctly measured compared to 57% for grayscale images.

X-rays have also been successfully used to detect lumber quality defects. Schajer (2001) used a multi-channel X-ray scanner to determine wood density and to estimate the strength of 800 specimens of 2 × 4 southern pine lumber. The strength-estimation method algorithm detected the location of knots by identifying high-density areas within the lumber. The relationship between strength values obtained through destructive testing versus estimated via the X-ray scanner had a coefficient of determination (R^2) between 0.68 and 0.78. The bending-stiffness R^2 values were between 0.50 and 0.60. The authors suggested that X-rays could more effectively describe strength properties of the tension and compression zones of lumber, and with the increase in strength prediction accuracy could directly translate to higher yields of stress-rated products.

Oh et al. (2009) used a single-pass X-ray machine to calculate the knot depth ratio (KDR) of lumber. Knot depth ratio is the ratio of the knot thickness to the thickness of the piece of lumber. The transition zone (TZ) is the area immediately surrounding knots and was included in the calculation of KDR because of similar density as knots. They tested 35 specimens of Japanese larch (*Larix kaempferi*) and 43 specimens of Japanese red pine (*Pinus densiflora*). The dimensions of each specimen were 38 mm thick 140 mm width by 3600 mm length. To test the effectiveness of the X-ray system, the measurement of the real KDR was obtained by overlaying cross-section areas that contained knots with a 1.31 × 1.31 mm mesh grid and counting the number of cells within the knot, TZ, and clearwood. They found that this method could accurately calculate the KDR with R^2 values of 0.87 and 0.83 for Japanese larch and red pine, respectively. The discrepancies between the predicted KDR and the measured KDR came from the very-small-diameter knots and cracks within the larger knots.

Oh et al. (2010) used X-rays to analyze the effects of knot adjacency on lumber strength. A total of 121 Japanese larch and 145 specimens of red pine were tested. These species were chosen because Japanese larch has multiple smaller knots while red pine has fewer but larger knots. They then conducted four-point bending setup in third-point loading static bending testing in accordance to ASTM International D198 (2014) on the red pine specimens. Center-point loading was conducted on the larch because of the difficulty in predicting a possible point of failure due to the abundance of smaller knots. Knots located within 150 mm of one another were considered as adjacent knots because South Korean visual grading standards consider those knots as clusters. The knot depth ratio (KDR) was calculated for each piece through x-ray image analysis according to Oh et al. (2009) methods. A linear model predicting MOR using KDR and knot adjacency as the two predictor variables had a R^2 of 0.59 and a RMSE of 8.57 MPa for Japanese larch and a R^2 of 0.53 and RMSE of 7.59 MPa for red pine.

Microwaves have also been successfully used to detect knots in lumber. Baradit et al. (2006) developed a technique to attain and process knot data by identifying how microwaves interact with the water within the wood. Kol and Yalcin (2015) used microwaves and dielectric parameters to predict strength of Nordmann fir (*Abies nordmanniana*) and sessile oak (*Quercus petraea*). The relationship between MOR and dielectric properties for Nordmann fir was R^2 = 0.47, and 0.77 for sessile oak. A similar trend was found with MOE (R^2= 0.42, R^2=0.71, respectively). However, the authors state that even with the high correlation between dielectric properties and wood strength, the non-homogeneous nature of wood as a material can possibly limit the commercial applicability of this method.

Arriaga et al. (2014) compared the measurements obtained from vibrating lumber longitudinally (L) and transversely (T) to predict MOE. Approximately 150 80×120 mm radiata pine (*Pinus radiata*) construction grade lumber pieces were tested. The natural longitudinal vibrations were recorded parallel to grain and obtained through two nodal points at each end of the lumber. The effects of the knots on lumber vibration was determined through two approaches. The first approach determined the relative knot diameter (RKD) which is the diameter of the knot divided by width or thickness of the lumber. The second approach was to determine the concentrated knot diameter ratio (CKDR). The CKDR is the sum of the KDRs within any given 15 cm length of a piece of lumber. The first approach provided a statistically significant result but had low coefficient of determination values between MOR and RKD (R^2 = 0.14). The second approach also yielded a statistically significant result between MOR and CKDR with an R^2 = 0.26. The result of implementing variable local defects improved the R^2 by 18%, however the results suggest were not very accurate at predicting MOR.

References

Abe H, and Funada R (2005) Review-The orientation of cellulose microfibrils in the cell walls of tracheids in conifers. IAWA J 26(2):161-174

Albaugh TJ, Allen HL, Fox TR (2007) Historical patterns of forest fertilization in the southeastern United States from 1969 to 2004. S J Appl Forest 31(3):129-137

Amateis R (2000) Modeling response to thinning in loblolly pine plantations. S J Appl Forest 24(1): 17-22

Amateis RL, and Burkhart HE (2012) Rotation-age results from a loblolly pine spacing trial. S J Appl Forest 36(1):11-18

Antony F, Schimleck LR, Clark A III, Daniels RF (2010) A multivariate mixed model system for wood specific gravity and moisture content of planted loblolly pine stands in the southern United States. 2010 Joint Meeting of Forest Inventory and Analysis (FIA) Symposium and the Southern Mensurationists

Arriaga F, Monton J, Segues E, Íňguez-Gonzales G (2014) Determination of the mechanical properties of radiata pine timber by means of longitudinal and transverse vibration methods. Holzforschung 68(3):299-305

ASTM International (2006) ASTM D245: standard practice for establishing structural grades and related allowable properties for visually graded lumber. ASTM International, West Conshohocken

ASTM International (2014) ASTM D198-14: standard test methods of static tests of lumber in structural size. ASTM International, West Conshohocken

Bailey RL (1986) Rotation age and establishment density for planted slash and loblolly pines. S J Appl Forest 10(3):162-168

Baradit E, Aedo R, Correa J (2006) Knot detection in wood using microwaves. Wood Sci Tech 40(1):118-123

Barnett JR, and Bonham VA (2004) Cellulose microfibril angle in the cell wall of wood fibres. Bio Rev 79(2):461-472

Borders BE, and Bailey RL (2001) Loblolly pine-pushing the limits of growth. J Appl Forest 25(2):69-74

Borders BE, Will RE, Markewitz D, Clark A, Hendrick R, Teskey RO, Zhang Y (2004) Effect of complete competition control and annual fertilization on stem growth and canopy relations for a chronosequence of loblolly pine plantations in the lower coastal plain of Georgia. Forest Ecol Manag 192(2004):21-37

Borders B, and Volfovicz, R (2012) Impact of cultural treatments and planting density on branch characteristics of Loblolly pine at seven and eight years of age. PMRC Tech. Rep. 2010-2, University of Georgia, Warnell School of Forestry and Natural Resources

Burdon RD, Kibblewhite RP, Walker JCF, Megraw RA, Evans R, Cown DJ (2004) Juvenile versus mature wood: a new concept, orthogonal to corewood versus outderwood, with special reference to Pinus radiata and P. taeda. Forest Sci 50(4):399-415

Butler MA, Dahlen J, Eberhardt TL, Montes C, Antony F, Daniels RF (2017) Acoustic evaluation of loblolly pine tree and lumber-length logs allows for segregation of modulus of elasticity, not modulus of rupture. Ann For Sci (2017) 74:20

Carter MC, Kellison RC, Wallinger RS (2015) Forestry in the U.S. South. Chapter 1. Louisiana State University Press.

Carter P, Chauhan S, Walker J (2006) Sorting logs and lumber for stiffness using Director HM200. Wood Fiber Sci 38(1):49-54

Chan JM, Walker JC, Raymond CA (2011) Effects of moisture content and temperature on acoustic velocity and dynamic MOE of radiata pine sapwood boards. Wood Sci Technol 45(4):609-626

Chase CW, Kimsey MJ, Shaw TM, Coleman MD (2016) The response of light, water, and nutrient availability to pre-commercial thinning in dry inland Douglas-fir forests. Forest Ecol Manag 363(2016): 98-109

Clark A, and Saucier JR (1989) Influence of initial planting density, geographic location, and species on juvenile wood formation in southern pine Forest Prod J 39(7/8):42-48

Clark A III, Daniels RF, Jordan L (2005) Juvenile/Mature wood transition in loblolly pine as defined by annual ring specific gravity, proportion of latewood and microfibril angle. Wood Fiber Sci 38(2):292-299

Clark A III, Jordan L, Schimleck L, Daniels RF (2008) Effect of initial planting spacing on wood properties of unthinned loblolly pine at age 21. For Pro J 58(10):78-83

Coble DW, and Grogan JB (2016) Effects of first thinning on growth of loblolly pine plantations in the west gulf coastal plain. SRS-212. USDA, Forest Service

Cramer S, Kretschmann D, Lakes R, Schmidt T (2005) Earlywood and latewood elastic properties in loblolly pine. Holzforschung 59(5):531-538

Davies NT, Altaner CM, Apiolaza LA (2016) Elastic constants of green Pinus radiata wood. New Zeal J For Sci (2016):46-19

Donaldson L (2008) Microfibril angle: measurement, variation and relationships- a review. Int Assoc Wood Anat 29(4):345-386

Eberhardt TL, and Samuelson LJ (2015) Collection of wood quality data X-ray densitometry: a case study with three southern pines. Wood Sci Tech 49(4):739-753

Erikson RG, Gorman TM, Green DW, Graham D (2000) Mechanical grading of lumber sawn from small-diameter lodgepole pine, ponderosa pine, and grand fir trees from northern Idaho. Forest Prod J 50(7/8):59-65

Faust TD, Clark A, Courchene CE, Shiver BD, Belli ML (1999) Effect of intensive forest management practices on wood properties and pulp yield of young, fast growing Southern pine.

International Environmental Conference Preceding's April 18-21, 1999, Nashville, Tenn (2):501-512

Fortson JC, Shiver BD, Shackelford L (1996) Removal of competing vegetation from established loblolly pine plantations increases growth on Piedmont and Upper Coastal Plain sites. S J Appl Forest 20(4):188-193

Fox TR, Allen HL, Albaugh JT, Rubilar R, Carlson CA (2007a) Tree nutrition and forest fertilization of pine plantations in the Southern United States. S J Appl Forest 31(1):5-11

Fox TR, Jokela EJ, Allen HL (2007b) The development of pine plantation silviculture in the southern United States. J For 105(7):337–347

Galligan WL, McDonald KA (2000) Machine grading of lumber: Practical concerns for lumber producers. FPL-GTR-7. USDA, Forest Service

Gartner BL (2005) Assessing wood characteristics and wood quality in intensively managed plantations. J Forest 103(2):75-77

Grabianowski M, Manley B, Walker J (2006) Acoustic measurement on standing trees, logs, and green lumber. Wood Sci Tech 40(3):205-216

Gräns D, Isik F, Purnell RC, McKeand SE (2016) Genetic variation in response to herbicide and fertilization treatments for growth and form traits in loblolly pine. Forest Sci 62(6):633-640

Hennessey T, Dougherty P, Lynch T, Wittwer R, Lorenzi E (2004) Long-term growth and ecophysiological responses of a southeastern Oklahoma loblolly pine plantation to early rotation thinning. Forest Ecol Manag 192(1):97-116

Isik F, Goldfarb B, Lebude A, Li B, McKeand S (2005) Predicted genetic gains from testing efficiency from two loblolly pine clonal trails. Can J Forest Res 35(7):1754-1766

Jain AK, and Dubes RC (1988) Algorithms for clustering data. Prentice Hall

Jain AK (2010) Data clustering: 50 years beyond K-means. Pattern Recogn Lett 31(8):651-666

Jokela EJ, and Long AJ (2000) Using soils to guide fertilizer recommendations for southern pines. UF Institute for Food and Agricultural Sciences 13pp

Jokela EJ, Wilson DS, Allen JE (2000) Early Growth Responses of Slash and Loblolly Pine Following Fertilization and Herbaceous Weed Control Treatments at Establishment. S J Appl Forest 24(1):23-30

Jokela EJ, Martin TA, Vogel JG (2010) Twenty-five years of intensive forest management with southern pines: important lessons learned. J Forest 108(7):338-347

Jordan L, He R, Hall, DB, Clark A III, Daniels RF (2006) Variation in loblolly pine cross-sectional microfibril angle with tree height and physiographic region. Wood Fiber Sci 38(3): 390-398

Jordan L, He R, Hall, DB, Clark A III, Daniels RF (2007) Variation in loblolly pine ring microfibril angle in the southeastern United States. Wood Sci Tech (39(2): 352-363

Jordan L, Clark A III, Schimleck LR, Hall DB, Daniels RF (2008) Regional variation in wood specific gravity of planted loblolly pine in the United States. Can J Forest Res 38(4): 698-710

Kanungo T, Netanyahu NS, Wu AY (2002) An efficient k-means clustering algorithm: analysis and implementation. IEEE T Pattern Anal 24(7):881-892

Kol HS, Yalçin Í (2015) Predicting wood strength using Dielectric parameters. BioResources 10(4):6496-6511

Kozlowski TT, Kramer PJ, Pallardy SG (1991) The physiological ecology of woody plants. San Diego, CA: Academic Press, pp. 258, 268-269

Larson PR (1969) Wood formation and the concept of wood quality. Yale University: School of Forestry Bulletin No. 74

Lasserre JP, Mason E, Watt M (2004) The influence of initial stocking on corewood stiffness in a clonal experiement of 11-year-old Pinus radiata D. Don. New Zeal For Sci 49(2): 18–23

Lenz P, Auty D, Achim A, Beaulieu J, Mackay J (2013) Genetic improvement of white spruce mechanical wood traits- early screening by means of acoustic velocity, Forests (2017) 4:575-594

Li B, McKeand S, Weir RJ (1999) Tree improvement and sustainable forestry — impact of two cycles of loblolly pine breeding in the U.S.A. Forest Gen 6(4):229–234

Likas A, Vlassis N, Verbeek JJ (2003) The global k-means clustering algorithm. Pattern Recogn 36(2):451-461

Lycken A (2006) Comparison between automatic and manual quality grading of sawn softwood. Forest Prod J 56(4):13-18.

Martin SW, and Shiver BD (2002) Impacts of Vegetation Control, Genetic improvement and their interaction on loblolly pine growth in the southern united states- Age 12 results. S J Appl Forest 26(1):37-42

McKeand S, Mullin T, Bryam T, White T (2003) Deployment of genetically improved loblolly and slash pines in the South. J Forest 101(3):32-37

Mei B, and Clutter ML (2014) Evaluating timberland investment opportunities in the United States: A real options analysis. Forest Sci 61(2):328-335

Mora CR, Schimleck LR, Isik F, Mahon JM Jr, Clark A III, Daniels RF (2009) Relationship between acoustic variables and different measures of stiffness in standing Pinus taeda trees. Can J Forest Res 39(8):1421-1429

Munsell JF, and Fox TR (2010) An analysis of the feasibility for increasing woody biomass production from pine plantations in the southern United States. Biomass Bioenerg 34(2010):1631-1642

Oh JK, Shim, K, Kim KM, Lee JJ (2009) Quantification of knots in dimension lumber using a single-pass X-ray radiation. J Wood Sci 55(4):264-272

Oh JK, Kim KM, Lee JJ (2010) Use of adjacent knot data in predicting bending strength of dimension lumber by x-ray. Wood and Fiber Sci 42(1):10-20

Pfeffer MJ, Francis JD, Ross Z (2006) Farmland Change, Urbanization and a changing farm economy. Occasional Policy Brief Series

Prats-Montalbán JM, Juan A, Ferrer A (2011) Multivariate image analysis: A review with applications. Chemometr Intell Lab 417(1-2):280-290

Rausher HM, and Johnsen K (2004) Southern forest science: past, present and future. Gen Tech Rep. SRS-75. USDA, Forest Service.

Raymond CA, Joe B, Anderson DW, Watt DJ (2008) Effect of thinning on relationships between three measures of wood stiffness in Pinus radiata: standing trees vs. logs. vs. short clear specimens. Can J Forest Res 38(11):2870-2879

Roblot G, Bléron L, Mériaudeau F, Marchal R (2010) Automatic computation of the knot area ratio for machine strength grading of Douglas-fir and Spruce timber. Eur J Environmental Civil Eng 14(10):1317-1332

Ross RJ, Geske EA, Larson GL, Murphy JF (1991) Transverse vibration nondestructive testing using a personal computer. FPL-RP-502. USDA Forest Service

Ross RJ (2015) Nondestructive evaluation of wood: second edition. General Technical Report FPL-GTR-238. USDA, Forest Service, Forest Products Laboratory, Madison, WI

Roth BE, Li X, Huber DA, Peter GF (2007) Effects of management intensity, genetics and planting density on wood stiffness in a plantation of juvenile loblolly pine in the southeastern USA. Forest Ecol Manag 246(2-3):155-162

Russ JC, and Russ JC (2007) Introduction to image processing and analysis. Boca Raton, FL: Taylor & Francis.

Schajer GS (2001) Lumber strength grading using X-ray scanning. Forest Prod J 51(1):43

Schultz RP (1997) Loblolly Pine: The Ecology and Culture of Loblolly Pine (Pinus taeda). USDA Agriculture Handbook, 713 pp.

Schultz RP (1999) Loblolly-the pine for the twenty-first century. New Forest 17:71-88

Siry JP (2002) Intensive timber management practices. GTR SRS-53. USDA, Forest Service pp. 327–340

Smook GA (2002) Hanbook for pulp and paper technologists. 3rd ed. Angus Wilde Publications Inc., Vancouver, B.C.

Sorensson C (2006) Varietal pines boom in the US South. New Zeal J For 51(2):34–40

Sword Sayer MA, Goelz J, Chambers J, Tang Z, Dean T, Haywood J, Leduc D (2004) Long-term trends in loblolly pine productivity and stand characteristics in response to thinning and fertilization in the West Gulf region. For Ecol Manag 192(1):71-96

Todoroki CL, Lowell EC, Dykstra D (2010) Automated knot detection with visual post-processing of Douglas-fir veneer images. J Comput Elect Ag 70(1):165-171

Vikram V, Cherry ML, Briggs D, Cress DW, Evans R, Howe GT (2011) Stiffness pf Douglas-fir lumber: effects of wood properties and genetics. Can J For Res 41:1160-1173

Wang X, Carter P, Ross RJ, Bradshaw BK (2007) Acoustic assessment of wood quality of raw forest materials- a path to increased profitability. For Prod J 57(5):6-14

Wear DN, and Greis JG (2002) Southern forest resource assessment: Summary of findings. J Forest 100(7):6-14

Weng T, Ford R, Tong Z, Krasowski M (2017) Genetic parameters for bole straightness and branch angle in jack pine estimated using linear and generalized mixed models. Forest Sci 63(1):11-17

Williamson GB, and Wiemann MC (2010) Measuring wood specific gravity… correctly!. Am J Bot 97(3):519-524

Xiong JS, McKeand SE, Whetten RW, Isik FT (2014) Genetics of stem forking and ramicorn branches in a cloned loblolly pine family. Forest Sci 60(2):360-366

CHAPTER 3: MAPPING THE EFFECTS OF KNOTS ON LOBLOLLY PINE LUMBER[1]

[1]Wright, S.L., Dahlen J., Montes, C., Eberhardt T.L. To be submitted to Wood Science and Technology.

Abstract

Loblolly pine (*Pinus taeda*) plantation rotation lengths are shifting from 35-40 to 22-25 years due to the implementation of intensive forest management. Lumber extracted from younger plantations will tend to have lower stiffness (modulus of elasticity (MOE)) and strength (modulus of rupture (MOR)) than lumber from older plantations. This study analyzed the knots of dimension lumber sourced from intensively managed 24-33-year-old trees harvested from the Lower Coastal Plain in Georgia. The aim of the research was to develop a rapid method to evaluate knots and develop models that predict stiffness and strength. The methodology involved lumber image evaluation using a semi-automated process using K-means clustering to identify the knots from the clearwood on 2×6 and 2×8 lumber. For each piece of lumber, a rectangle was overlaid on to each knot with the summed rectangle areas divided by the total surface area of the lumber to calculate the knot area ratio (KAR). Lumber stiffness was best modeled using KAR and dynamic MOE; the linear model had a R^2 of 0.69 with RMSE of 1.29 GPa. The variation in lumber strength was best described by KAR and MOE_{dyn} which yielded an R^2 of 0.53 with a RMSE of 8.47 MPa. Significant differences were found in MOR when lumber was classified into three failure type categories: in clearwood, at a single knot, and at combination of knots.

1 Introduction

The southeastern United States has become one of the most important regions for lumber production due to abundant raw material availability through extensive replanting of abandoned agricultural fields with major southern pine species including loblolly pine (*Pinus taeda*), longleaf pine (*Pinus palustris*), shortleaf pine (*Pinus echinata*) and slash pine (*Pinus elliotii*) (Schultz 1999; Wear and Greis 2002; Pfeffer et al. 2006; Fox et al. 2007a). Wear and Greis (2002) estimated that the region's timber production doubled between 1952 and 1997 and its share of the world's lumber production increased from 6.3 to 15.8%. The increase in timber production is mostly attributed to growth in pine plantations, with later increases attributed to intensive forest management (IFM) practices in those plantations (Jokela et al. 2009). Factors including competition control, improved genetics and fertilization have accelerated plantation growth to where sawtimber size trees (DBH ≥ 31 cm) can be achieved at age 25 and chip-n-saw size trees (DBH ≥ 23 cm DBH ≤ 30 cm) can be achieved in 16 years (Clark et al. 2008; Vance et al. 2010). These increased growth rates have resulted in wood with lower specific gravity (SG), lower percentage of latewood, higher corewood percent compared to outerwood, and higher microfibril angle (MFA) (Faust et al. 1999; Burdon et al. 2004; Cramer et al. 2005; Clark et al. 2008).

One of the most important products produced from softwoods is dimension lumber (Howard 2006). The increase in corewood from trees harvested from young plantations has been shown to play an important role in reducing lumber stiffness (modulus of elasticity (MOE)) and strength (modulus of rupture (MOR)) (Barnett and Bonham 2004; Biblis 2006). Within lumber, knots are one of the most serious characteristics that affect strength and stiffness (Oh et al. 2009). Lumber failure occurs around the weakest cross section, which is often at a knot or near knots because of severe grain deviation around the knots (Madsen 1992). To account for the impact of knots on lumber properties, the lumber industry has developed methods for separating lumber into strength categories based on visual analysis of lumber characteristics such as knots, pitch and wane (ASTM International 2006). Visual grading is based on the examination of the four faces of lumber in which the size and nature of knots and other defects are evaluated (ASTM International 2006). Allowable knot sizes for the No. 1 and No. 2 grade 2×6 and 2×8 sizes are shown in Table 1.

Table 3.1 Allowable knot sizes by lumber size and number for visually graded lumber.

Size	Grade	Edge Knot (cm)	Centerline Knot (cm)
2 × 6	No. 1	3.8	5.7
	No. 2	4.8	7.3
2 × 8	No. 1	5.0	7.0
	No. 2	6.4	8.9

Studies have successfully used a wide range of technologies to identify and analyze knots. Roblot et al. (2010) used optical scanners to automatically detect knots in Douglas-fir (*Pseudotsuga menziesii*) and spruce-fir (*Picea excelsa*) dimension lumber. The identification of the knots allowed for the computation of the knot area ratio (KAR) which is the cross-sectional area of the knots divided by the total lumber area. Predicting MOR from KAR and other explanatory variables including ring width, density and MOE explained 42% to 72% of the variation in MOR (RMSE not reported). Schajer (2001) successfully used an X-ray scanner to estimate wood density of 2×4 southern pine lumber. A 0.67 to 0.78 R^2 was found between destructively measured strength and estimated lumber strength. Oh et al. (2009) used a single pass X-ray machine to calculate the knot depth ratio (KDR). The KDR is calculated as the depth of the knot divided by the thickness of the lumber. The R^2 between measured and predicted KDR was 0.87 for Japanese red larch (*Larix kaempferi*) and 0.83 for Japanese red pine (*Pinus densiflora*) (RMSE not reported).

The increase in computing power has allowed image analysis to rapidly advance many fields including agriculture, botany and medical (Downie et al. 2015; Mayer et al. 2017; Zaborowicz et al. 2017). Images are an array of pixels referenced by coordinate values (x,y). The x value indicates the distance from the left edge of the image and the y value indicating the distance from the top of the image. Each pixel in a red, green and blue (RGB) scale image has three layers of data with each layer corresponding to a single-color band. This allows for each layer to represent a segment of the electromagnetic spectrum. Each of the three layers is encoded as a number in a range between 0 and 255, with 0 representing darkness and 255 representing brightness (Russ and Russ 2007).

Recent changes in design values for southern pine lumber in conjunction of wider implementation of IFM practices increases the need to evaluate the raw material supply chain to further understand the mechanical properties of lumber being milled today. Likewise, a cost-effective laboratory method of evaluating knots needs to be developed to better understand the relationship between knots and IFM. A better understanding of the interaction between IFM and lumber quality could lead to improved management decisions such silvicultural regimes, raw material sourcing, and lumber grading. The objectives of this study were to (1) develop a laboratory grade knot image analysis system, (2) identify the relationship between the knot area ratio (KAR) and lumber stiffness and strength, (3) to investigate if knot information plus other non-destructive measurements of wood quality can predict lumber stiffness and strength, and (4) determine the influence of failure type on the mechanical properties of lumber.

2 Materials and methods

2.1 Lumber source

Trees used in this study were harvested from productive stands in the Lower Coastal Plain near Brunswick, GA (Butler et al. 2016). Stands selected for harvest had site indices (SI_{25}) between 25 m to 27 m. In total, 93 loblolly pine trees were harvested. All stands were being thinned at least once, and had been site-preparation, fertilization (NPK), and received woody and herbaceous control. The stands were established using genetically improved seedlings with an initial stocking of approximately 1,550 trees per hectare. The specific number of trees being selected at each plot for harvest was based on 2.5 cm diameter classes derived from the average diameter size distribution across the whole stand. Trees were felled, delimbed, and bucked into 5.2 m logs in the woods prior to transport. At the mill, the logs were sawn into 2×4, 2×6, 2×8 and 2×10 lumber. Only 2×6 and 2×8 lumber images were used in this study. The lumber was kiln-dried, planed and assigned grades by certified graders.

2.2 Image source

After the logs had been processed at a sawmill, the lumber was transported to the Wood Quality Laboratory at the University of Georgia in Athens, GA. The lumber was then cut into the appropriate test span, length which was 17 times the depth of the lumber (ASTM International 2013). Physical attributes of each piece of lumber such as width, length, thickness, specific gravity (SG) and acoustic velocity (AV) using the Director HM200 (Fibre-gen, Christchurch, New Zealand) was measured. The cut-to-span pieces of lumber were subjected to four-point static bending in accordance to ASTM D198 (ASTM International 2014) and ASTM D4761 (ASTM International 2013) standards. The MOE was determined from the displacement of the lumber caused by the applied load in the linear region and MOR was determined from the total amount of load applied at the moment of failure. The length to failure and type of failure (tension, compression, shear, and combination) were recorded following testing.

2.3 Image analysis software

Knot detection, statistical analysis and associated graphics were completed using R 3.3.1 (R Core Team 2017) with RStudio v0.99.893 interface (RStudio 2017) and the packages raster (Hijams 2016), maps (Brownrigg 2016), sp (Pebesma and Bivand 2016), rgdal (Bivand et al. 2017), rgeos (Bivand and Rundel 2017) and tidyr (Wickham 2017). The Python programming language (Rossum 2007), GIMP 2.8.16 (GIMP Team 2012) and Fiji (Schindelin et al. 2012) were also used for image preparation.

2.4 Knot data collection

There were 71 2×6's photographed on both sides, with 13 No. 1 and 58 No. 2 pieces of lumber. A total of 99 2×8's lumber pieces were photographed on both sides, with 59 No. 1 and 40 No. 2 pieces of lumber. A hybrid system which relied on a combination of algorithms and human selection was developed for detecting the knots (Figure 1). The region of interest within the lumber was first determined, then a white mask was applied to isolate the lumber from the background. Next, a polynomial transformation was conducted on each image by subtracting the maximum component value of each band from every component value then multiplied by the maximum component value for an 8-bit image (255) divided by the difference between the maximum and minimum component value for each layer. The polynomial transformation effectively removed the effects of the camera flash and equalized the contrast. K-means clustering was then used to identify knotty regions of the lumber. K-means clustering is a self-learning algorithm that minimizes the mean squared distance from each data point to each k center (Hartigan and Wong 1979, Kanungo et al. 2002). The knot size and position coordinates were then determined based on the pixel dimension and location contained within each knot.

After the knots were identified, a manual selection and revision was carried out to ensure that the selected areas corresponded to actual knots. The image distortion was corrected in Python by applying a projective transformation, which identified the corner coordinates of each image and stretched them to undistorted coordinates (Hartley and Zisserman 2003) (Figure 2).

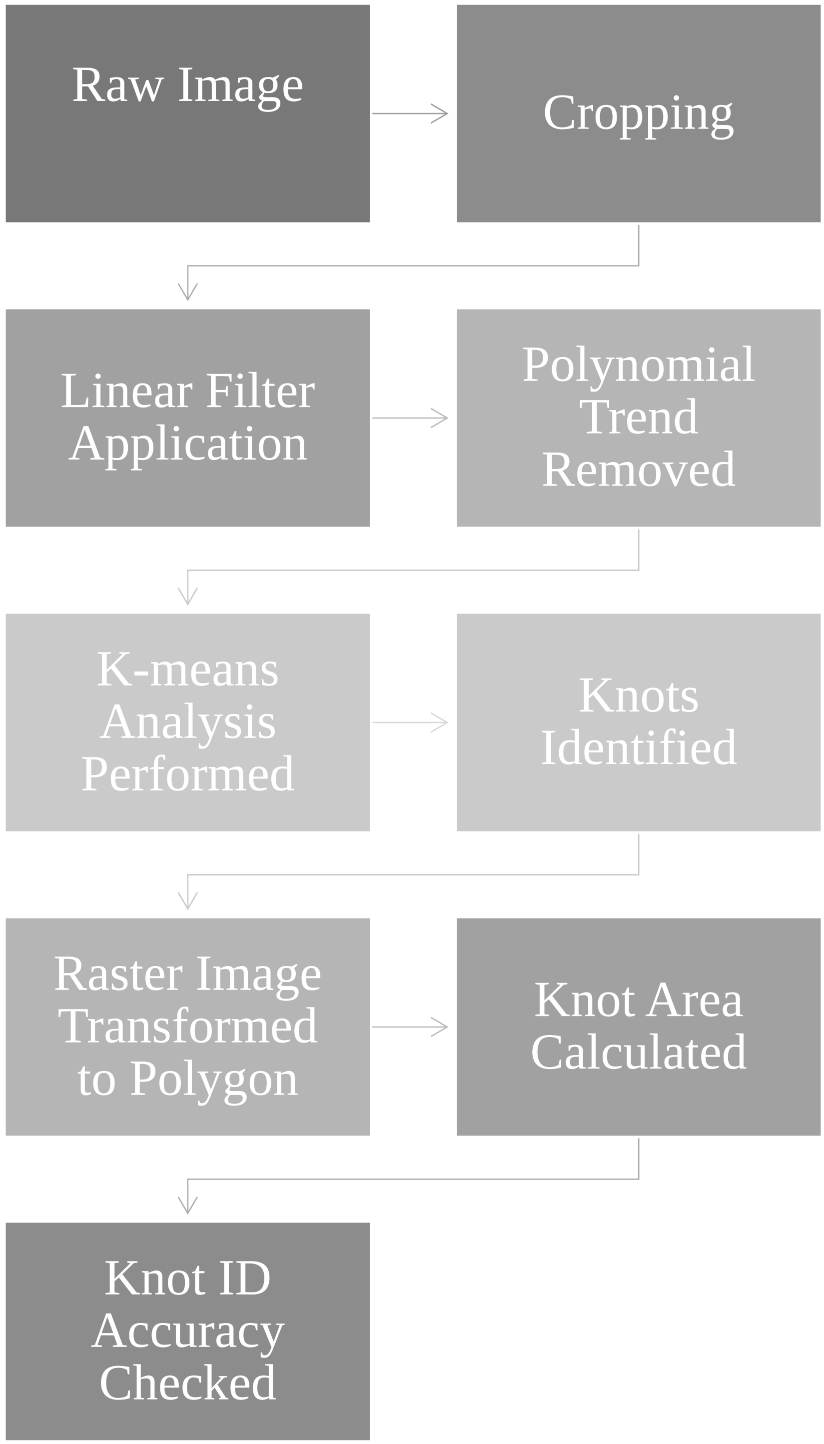

Fig. 3.1 The image analysis workflow performed on each piece of lumber containing knots.

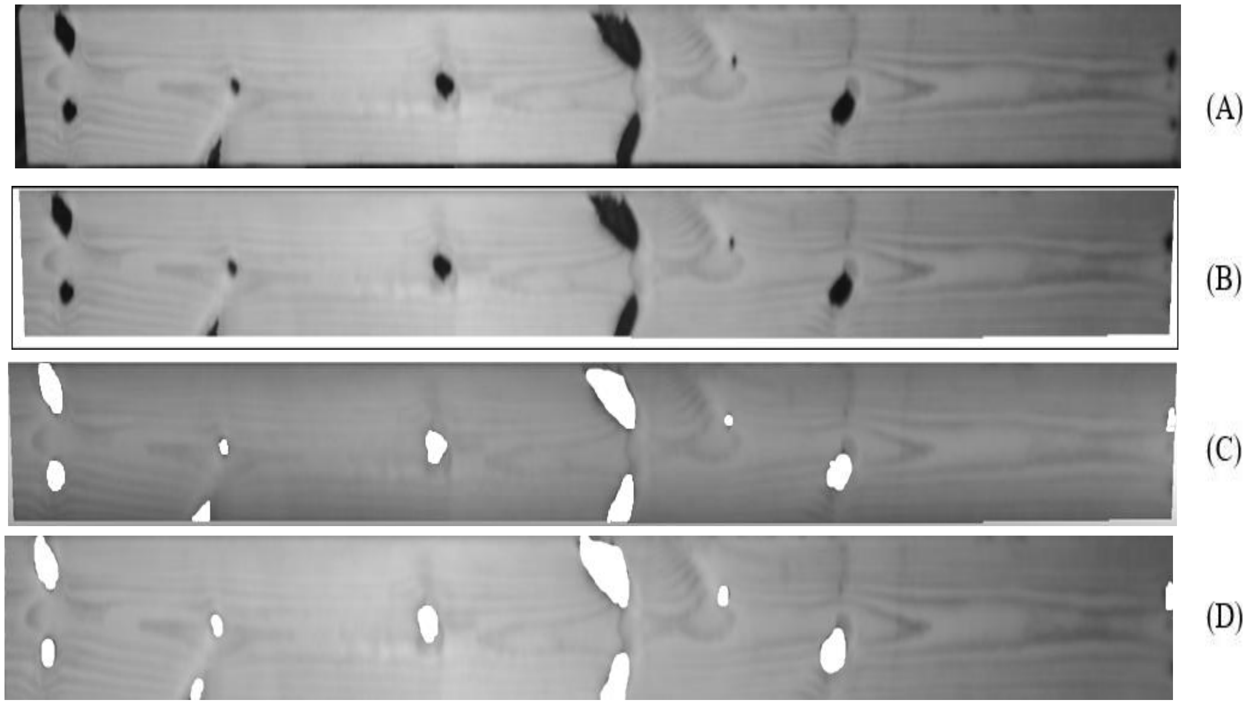

Fig. 3.2 Example of image processing and analysis method of lumber. Image (A) is the rough cropped image. Image (B) is the rough cropped image with a white mask applied. Image (C) shows the lumber with the initial knot detection, and image (D) shows an image with the distortion removed.

2.5 Knot Area Ratio Measurements

We defined the KAR as the cross-sectional area of the knot divided by the total lumber cross section area (Roblot et al. 2010). The KAR was chosen as the method of quantifying the knots because it is a simple measure, accounts for the surface area of every knot and has successfully been used in previous work (Lam et al. 2003; Lam et al. 2004; Roblot et al. 2010). Actual KAR (KAR_{actual}) was calculated by summing the total area of the knots for both sides of the lumber and then dividing the sum by the total area of the lumber. The rectangular KAR ($KAR_{rectangle}$) was measured by finding the maximum and minimum y and x values of each knot, and then converting these coordinates to a rectangle. The $KAR_{rectangle}$ was then calculated by summing the area of each rectangle and dividing the summed area by the total lumber area. The knot quantification methods were compared to determine if one method was more accurate than the other (Figure 3).

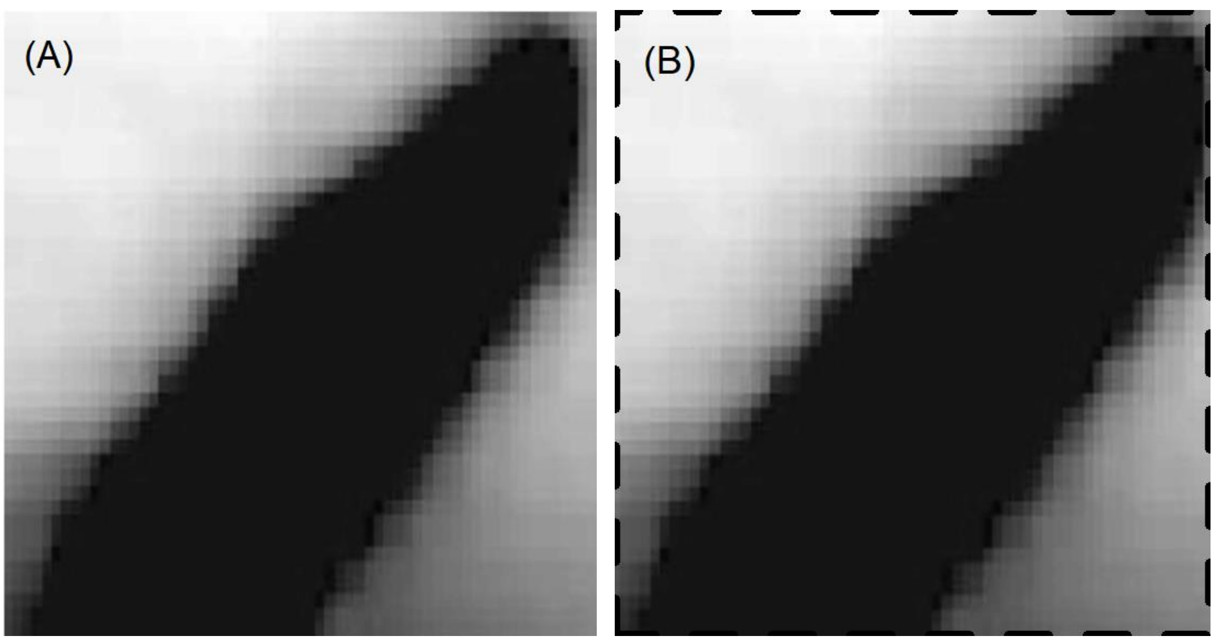

Fig. 3.3 (A) refers to KAR_{actual} where only the black area is considered and (B) refers $KAR_{rectangle}$ where the whole area encompassed in the dotted rectangle.

2.6 Additional non-destructive Variables

Acoustic velocity was calculated by measuring the frequency of multiple acoustic pulses on each piece of lumber using the Director HM200 (Fibre-gen, Christchurch, New Zealand). The specific gravity (SG) of each piece of lumber was calculated from the weight, dimensions and moisture content. The dynamic lumber stiffness (MOE_{dyn}) was calculated using:

$$Dynamic\ MOE = \frac{AV^2 * density}{1{,}000{,}000{,}000} \tag{1}$$

where AV is the acoustic velocity in meters/second, density in kg/m^3, and MOE in GPa.

2.7 Regression analysis using KAR and non-destructive lumber quality measurements

Linear regression was used to test multiple models using KAR_{actual}, $KAR_{rectangle}$, AV, SG, and MOE_{dyn}. Model fit was evaluated using R^2, root-mean-square-error (RMSE), and partial R^2. A square root transformation was applied to both KAR measurements to transform the relationship between MOE, MOR and KAR from negative curvilinear to a negative linear relationship.

The following linear models were proposed using the least squares approach:

$$y = \beta_0 + \beta_1 \times \sqrt{KAR} + \beta_2 \times NDE + \in \tag{2}$$

where y is the dependent variable (MOE or MOR), β_0, β_1, and β_2 are calculated parameters, KAR is either KAR_{actual} or $KAR_{rectangle}$ and NDE is either AV, SG or MOE_{dyn}. The RMSE of each model was calculated using:

$$RMSE = \sqrt{\frac{\sum(y_i - \hat{y})^2}{n - p}} \tag{3}$$

where y_i is the predicted value, $\hat{y}$ is the observed value, n is sample size and p is the number of parameters. The partial R^2 shows the additional amount of variability explained by adding explanatory variables in a complete model versus a reduced model. It is calculated using:

$$R^2_{partial} = \frac{SSE_r - SSE_c}{SSE_r} \quad (4)$$

here SSE_r is sum of squares errors of prediction for the reduced model and SSE_c is the sum of squares errors of prediction for the complete model.

2.8 Lumber failure

Location of lumber failure data was recorded and converted from centimeters to the local coordinate system of the images (pixels) by dividing the length of each image by the length of each piece of lumber and then multiplying that value by the location of failure. Following graphing the location of failure for each image, the lumber was classified into three different types of failure. The first type was lumber that failed at clearwood (CWF), the second type failed at a knot (KF), and the third type of failure was the combination knot failure (CKF). Combination knot failure occurred when it was evident that lumber failure was caused by two or more consecutive knots on the wide face of the lumber. One-way analysis of variance (ANOVA) at a 0.05 significance level was used to determine significant differences in the means of MOR, MOE, KAR, SG and AV for the three different groups of failure. If the ANOVA proved that there was a significant difference in the means, a Tukey's test was used to determine the difference in means ($\alpha = 0.05$) between specific types of failure.

3 Results and discussion

3.1 Summary Statistics

Summary statistics for relevant variables are presented in Table 2. A one-way ANOVA and Tukey tests were conducted on the means of all the variables to determine statistically significant differences in means. For KAR, the only significant difference in the means was between No. 1 and No. 2 2 × 8 (p-value = 0.015). In the case of SG, there was a statistically significant difference between No. 1 and No. 2 2 × 8 (p = 0.039) and No. 1 2 × 6 and No. 1 2 × 8 (p = 0.011). The only significant difference for AV was between No. 2 2 × 6 and No. 2 2 × 8 (p = 0.048). The only significant difference for MOE_{dyn} was between No. 2 2 × 6 and No. 2 2 × 8 (p = 0.017). There was a difference in means between No. 2 2 × 6 and No. 1 2 × 8 (p = .042) and No. 1 2 × 6 and No. 1 2 × 8 (p = .018) for MOE. There was no statistically significant difference in the means for MOR between lumber size and grade.

Table 3.2 Summary statistics for the variables used in model development.

			KAR (%)			SG			AV (m/s)			MOEdyn (GPa)			MOE (GPa)			MOR (MPa)		
Siz	Grade	n	Mean	Std	Range	Mean	Std	Range	Mean	Std	Range	Mean	Std	Range	Mean	Std	Range	Mean	Std	Range
2x6	No. 1	12	1.29	0.4	1.2	0.53	0.05	0.18	4706	318	940	13.5	3	8.3	10.8	3	9.9	40.9	10	34.4
2x6	No. 2	58	1.88	0.7	3.2	0.50	0.05	0.20	4612	367	1640	12.2	3	12.3	10.1	2	9.4	37.0	12	48.6
2x8	No. 1	59	1.40	0.4	2.1	0.53	0.04	0.19	4594	305	1450	12.7	2	11.6	11.3	2	9.6	42.2	11	48.5
2x8	No. 2	40	2.08	0.7	2.7	0.50	0.05	0.18	4466	361	1770	11.4	2	10.4	10.1	2	9.0	36.7	13	51.5

3.2 Relationship between variables

There was a significant positive correlation between AV, SG and MOE_{dyn} (0.9, 0.75), which is expected because MOE_{dyn} is calculated from AV and SG (Table 3). The two KAR measurements were significantly correlated (0.97), which might explain the lack of difference in the performance of the reduced model using either KAR as the only prediction variable. There is a slight positive correlation relationship between AV and SG (0.4). Between both KAR measurements and AV (m/s), SG, MOE_{dyn} (GPa), there were strong negative correlations, ranging from -0.47 to -0.55.

Table 3.3 Pearson correlation matrix among lumber properties used to model stiffness and strength.

Property	AV (m/s)	SG	MOE_{dyn} (GPa)	KAR_{actual} (%)
AV (m/s)				
SG	0.40			
MOE_{dyn} (GPa)	0.90	0.75		
KAR_{actual} (%)	-0.47	-0.48	-0.55	
$KAR_{rectangle}$ (%)	-0.48	-0.48	-0.55	0.97

3.3 Lumber stiffness and strength modeling

There is an inverse relationship between MOR, MOE and $KAR_{rectangle}$ (Table 4; Figure 4). This trend is significant because it illustrates how an increase in KAR decreases the overall lumber strength and stiffness. These scatterplots also illustrate the amounts of variability between lumber MOR and MOE and KAR as solely determined by the wide faces of the lumber. For the lumber stiffness prediction, KAR was able to describe 30% of the variation with a RMSE value of 1.93 GPa. The lumber strength model using KAR was more successful at describing the variation in MOR than in MOE (R^2 = 0.38, RMSE = 9.70 MPa).

Table 3.4 Model performance for prediction of lumber stiffness and strength using KAR_{actual} and $KAR_{rectangle}$.

Model	R^2	RMSE
$MOE = 14.64 - 4.19 \times \sqrt{KAR_{actual}} + \in$	0.31	1.92 GPa
$MOE = 14.18 - 2.89 \times \sqrt{KAR_{rectangle}} + \in$	0.30	1.93 GPa
$MOR = 63.15 - 24.8 \times \sqrt{KAR_{actual}} + \in$	0.38	9.70 MPa
$MOR = 60.78 - 17.43 \times \sqrt{KAR_{rectangle}} + \in$	0.38	9.70 MPa

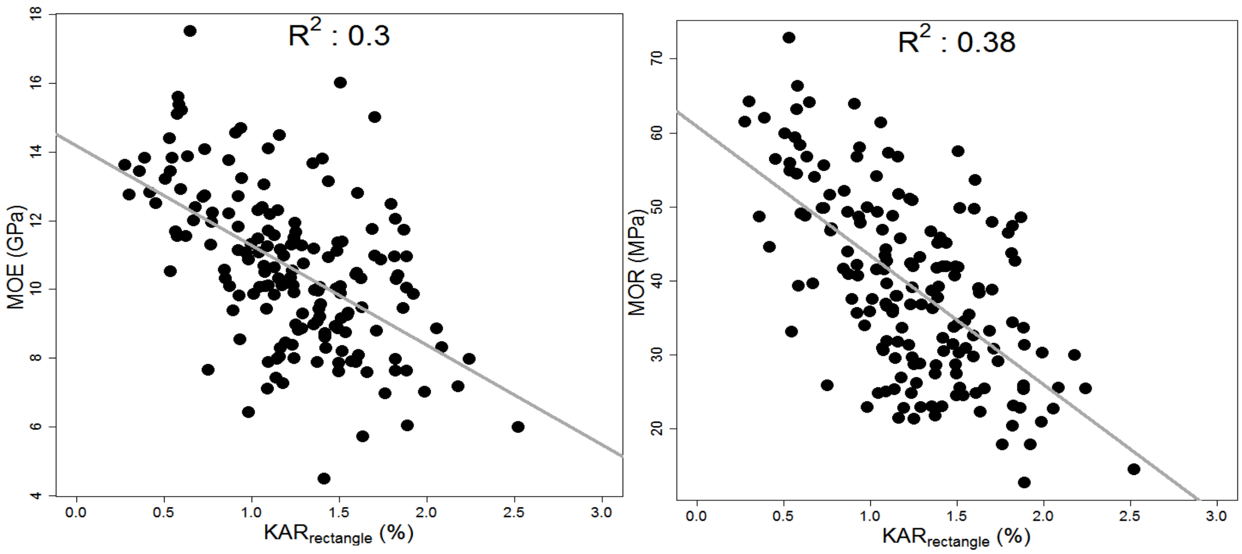

Fig. 3.4 The inverse relationship between square root $KAR_{rectangle}$ and modulus of elasticity and modulus of rupture.

For predicting MOE, adding AV to the model increased the model's ability to describe the variation in MOE by 19% (R^2 = 0.49), and it had a partial R^2 of 0.28 and decreased the RMSE to 1.64 GPa. The addition of SG to the reduced model increased the R^2 value by 0.33 versus the reduced model (R^2 = 0.63), increased the partial R^2 by 0.19 and decreased the RMSE to 1.41 GPa. Using MOE_{dyn} as the additional non-destructive variable to predict lumber stiffness yielded the best model performance but not the deemed to be the optimal model due to lack of significance at an alpha of 0.05. This model had the highest R^2 (0.69), highest partial R^2 (R^2 = 0.56) and the lowest RMSE (RMSE = 1.29 GPa) (Table 5, Figure 5).

Table 3.5 Prediction of modulus of elasticity using KAR and nondestructive lumber characteristics.

Equation	R^2	Partial R^2	RMSE (GPa)	Rank
$MOE = 14.18 - 2.89 \times \sqrt{KAR} + \epsilon$	0.30	--	1.93	4
$MOE = -2.93 - 1.53 \times \sqrt{KAR} + .0034 \times AV + \epsilon$	0.49	0.28	1.64	3
$MOE = -4.89 - 0.97 \times \sqrt{KAR} + 32 \times SG + \epsilon$	0.63	0.47	1.41	1
$MOE = 2.65 - 0.39 \times \sqrt{KAR} + 0.69 \times \mathrm{MOE_{dyn}} + \epsilon$	0.69	0.56	1.29	2

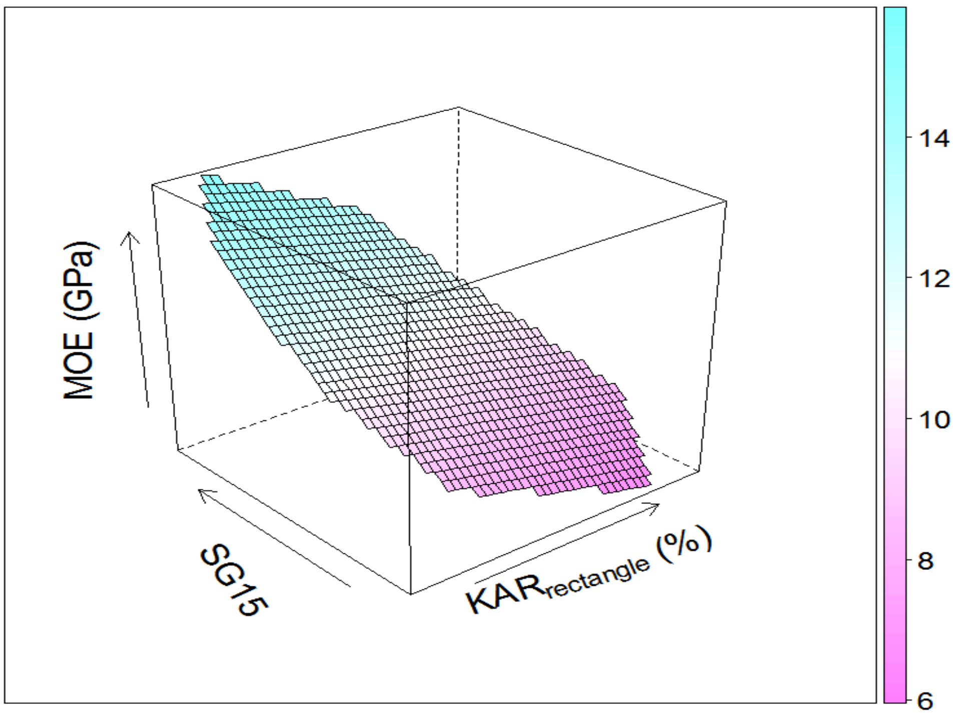

Fig. 3.5 Relationship between lumber stiffness, rectangle knot area ratio, and dynamic MOE with the regression pane from best model.

For predicting MOR, the addition of AV to the reduced model increased the R^2 to 0.45 while also decreasing the RMSE to 9.18 MPa. Specific gravity further increased the explanation in variability for lumber strength (R^2 = 0.53), increased the partial R^2 to 0.24 and decreasing RMSE to 8.53 MPa. The final complete model explored including MOE_{dyn} as the additional NDE variable. Dynamic MOE had the same R^2 as the model with SG (R^2 = 0.53), but it did slightly increase partial R^2 (partial R^2 = 0.25), and had the lowest RMSE value when compared to the other strength prediction models (RMSE = 8.47 MPa) (Table 6, Figure 6).

Table 3.6 Prediction of MOR using KAR_{actual} and nondestructive lumber characteristics.

Equation	R^2	Partial R^2	RMSE (MPa)	Rank
$MOR = 60.78 - 17.43 \times \sqrt{KAR} + \in$	0.38	--	9.70	4
$MOR = 5.79 - 13.11 \times \sqrt{KAR} + 0.011 \times AV + \in$	0.45	0.11	9.18	3
$MOR = -7.64 - 10.45 \times \sqrt{KAR} + 116.15. \times SG + \in$	0.53	0.24	8.53	2
$MOR = 22.24 - 9.1 \times \sqrt{KAR} + 2.3 \times \mathrm{MOE_{dyn}} + \in$	0.53	0.25	8.47	1

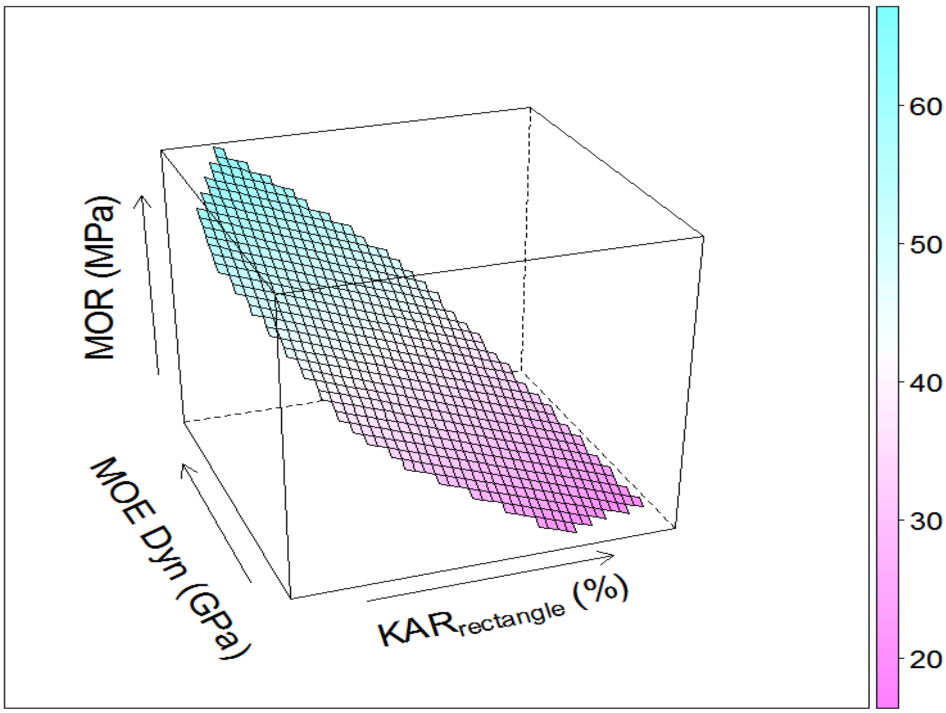

Fig. 3.6 Relationship between lumber strength, rectangle knot area ratio, and dynamic MOE with the regression pane from best model.

3.4 Lumber failure

The lumber was visually sorted into three groups based on location of failure. The groups were if failure occurred at clearwood, failed at a single knot, or failed at combination of knots. Examples of failure are shown in Figures 6-9. Results for MOR, MOE, KAR, SG and AV by lumber failure are shown in Table 7. There is a difference between the investigated lumber qualities based on type of lumber failure. By looking at the total number of pieces used in this study, 70 out of 168 failed directly at a knot while 72 and 26 failed in clearwood and combination knots, respectively. Lumber that failed at combination knots and in clearwood had much larger variance values and standard deviations in comparison to the variance and standard deviation values for lumber that failed at knot. This may be a result of not having an equal sample size across the three categories.

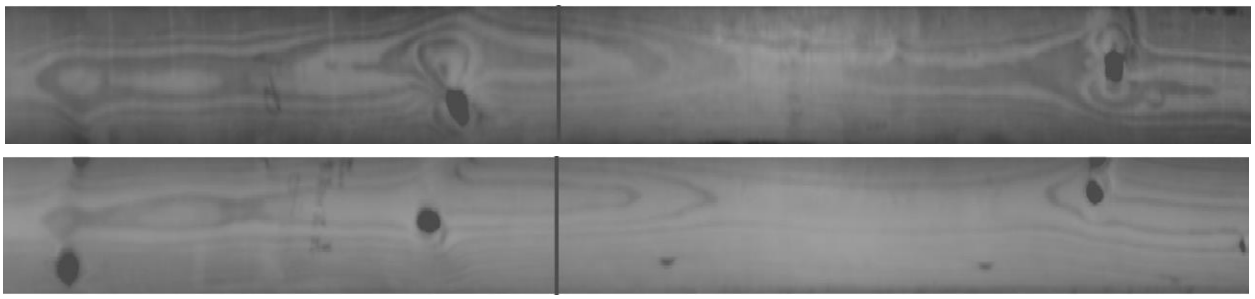

Fig. 3.7 Example of a 2 × 6 with the location of failure in clearwood.

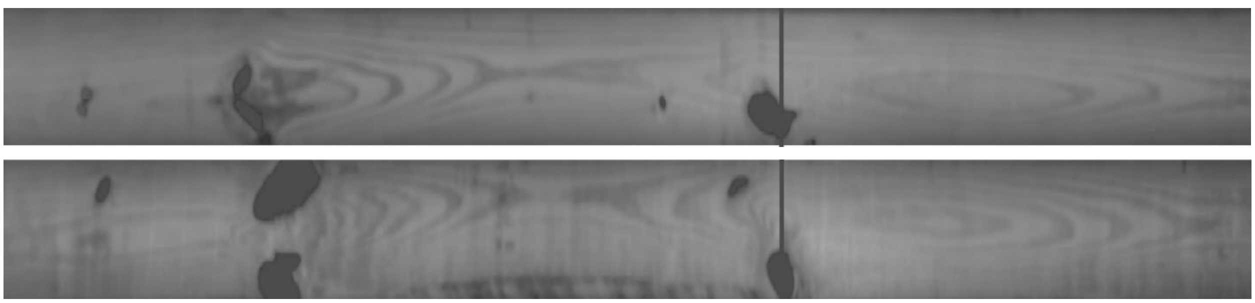

Fig. 3.8 Example of a 2 × 6 with the location of failure at a knot.

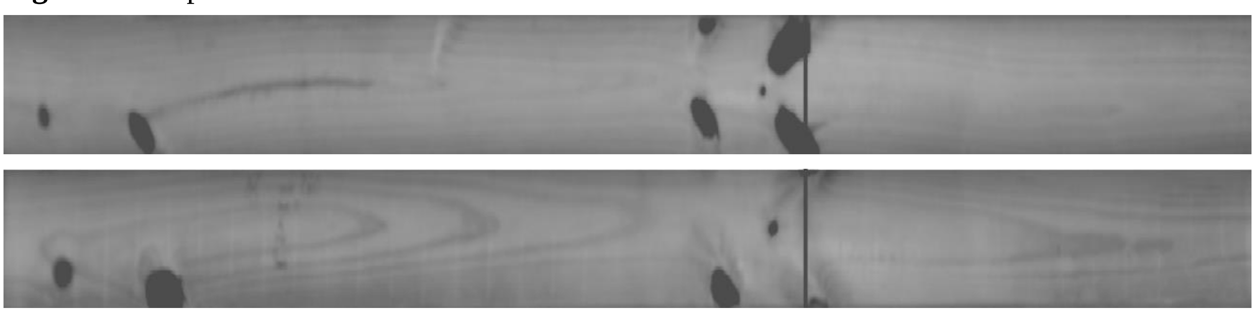

Fig. 3.9 Example of a 2 × 6 with the location of failure in at combination knots.

Table 3.7 Modulus of elasticity, modulus of rupture, $KAR_{rectangle}$, specific gravity and acoustic velocity values based on type of failure. Significant differences between the types of failure (α=0.05) indicated by letters.

Failure Type	Sample Size	Property	Range	Mean	Standard Deviation
Clearwood	N = 72	MOR(MPa)	51.5	43.8a	12.4
		MOE (GPa)	8.3	11.3a	2.10
		$KAR_{rectangle}$ (%)	3.9	7.9a	6.50
		SG	0.21	0.53a	0.048
		AV (m/s)	1910	4655a	364
At Knot	N = 70	MOR(MPa)	46.2	37.1b	11.1
		MOE (GPa)	13.0	10.4b	2.3
		$KAR_{rectangle}$ (%)	4.7	11.2b	5.88
		SG	0.22	0.50a	0.047
		AV (m/s)	1640	4,573b	330
Combo Knot	N = 26	MOR(MPa)	38.2	32.4b	11.04
		MOE (GPa)	8.1	9.48b	2.11
		$KAR_{rectangle}$ (%)	5.6	14.2b	6.60
		SG	0.13	0.49a	0.037
		AV (m/s)	1310	4409a	302

The ANOVA results of Table 7 showed that there were statistically significant differences in the means of MOR, MOE, $KAR_{rectangle}$, SG and AV for the three types of LF at a significance level of p = 0.05 and a critical F-value of 3.05 with 2 and 165 degrees of freedom (Table 7). The Tukey's post-hoc test revealed that for MOR, MOE, $KAR_{rectangle}$, and SG determination, there was a statistical difference between CWF and KF and CKF. For AV, the only statistically significant difference was found to be between CWF and CKF (Table 7). For the five measurements of lumber quality, lumber that failed in clearwood had the best mechanical properties. The statistically significant difference between CWF lumber and the other two types show that knots can play a significant part in the determination of mechanical properties. Lumber with large single knots or a high number of consecutive knots on the wide face of the lumber should be used carefully in their end use as to not accentuate the defects further.

There is a difference in the type of failure based on lumber size (Table 8). Nearly half of the 2 × 6's failed at a knot while a little more than a third of 2 × 8's failed at a knot. Lumber failure in combination knots was double for the smaller lumber verses the larger lumber. Overall, 55% of the lumber studied failed at a knot with 26 % failed in combination knots with a third failing in clearwood. The differences in the location can possibly be explained by multiple the factors. Because the larger lumber came from butt logs the knots were smaller but more numerous.

Table 3.8 Shows the breakdown of type of lumber failure based on lumber size.

	Type of Failure		
Size	At a Knot	Combination	Clearwood
2 × 6 (n = 69)	52%	22%	26%
2 × 8 (n = 99)	34%	11%	55%
Total (n = 168)	42%	15%	42%

Conclusions

A process to conduct cost-efficient knot analysis in a laboratory setting to predict the mechanical properties of lumber are presented here. Image analysis of loblolly lumber images was conducted using K-means clustering to identify knotty areas. Knots were quantified using KAR_{actual} and $KAR_{rectangle}$ where KAR_{actual} used the area of the knots, whereas $KAR_{rectangle}$ adheres more closely to lumber grading standards where knots are characterized as rectangles. Sixteen separate regression models were proposed to predict MOE and MOR using a measurement of KAR and other nondestructive variables: lumber specific gravity, acoustic velocity and dynamic lumber stiffness (MOE_{dyn}). The best performing model used the for the prediction of lumber stiffness the variables $KAR_{rectangle}$ and SG. The best model for predicting lumber strength included $KAR_{rectangle}$ with MOE_{dyn}. Using knot information along with other common measurements of lumber quality could lead to improved products by finding those knots that most negatively impact mechanical properties. As the knot area ratio increases, both lumber stiffness and strength decreased. Lumber that failed at a combination of knots had the lowest mechanical properties across the lumber.

References

ASTM International (2006) ASTM D245-06: standard practice for establishing structural grades and related allowable properties for visually graded lumber. ASTM International, West Conshohocken

ASTM International (2013) ASTM D4761-13: standard test methods for mechanical properties of lumber and wood-base structural material. ASTM International, West Conshohocken

ASTM International (2014) ASTM D1990-14: standard practice for establishing allowable properties for visually-graded dimension lumber from in-grade tests of full-size specimens. ASTM International, West Conshohocken

Barnett JR, and Bonham VA (2004) Cellulose microfibril angle in the cell wall of wood fibres. Bio Rev 79(2):461-472

Biblis EJ (2006) Flexural properties and compliance to visual grade requirements of 2 by 4 and 2 by 6 loblolly pine lumber obtained from a 19-year-old plantation. For Prod J 56(9):71-73

Bivand R, Keitt T, Rowlingson B (2017) rgdal: Bindings for the geospatial data abstraction library. R package version 1.2-7. https://cran.r-project.org/web/packages/rgdal/rgdal.pdf

Bivand R, and Rundel C (2017) rgeos: Interface to geometry engine- open source (GEOS). R package version 0.3-23. https://cran.rstudio.com/web/packages/rgeos/rgeos.pdf

Brownrigg R (2016) maps: Draw geographical maps. R package version 3.1.1. https://cran.r-project.org/web/packages/maps/maps.pdf

Burdon RD, Kibblewhite RP, Walker JCF, Megraw RA, Evans R, Cown DJ (2004) Juvenile versus mature wood: a new concept, orthogonal to corewood versus outderwood, with special reference to P. radiata and P. taeda. Forest Sci 50(4):399-415

Butler MA, Dahlen J, Daniels RF, Eberhardt TL, Antony B (2016) Bending strength and stiffness of loblolly pine lumber from intensively managed stands located on the Georgia Lower Coastal. Plain. Eur J Wood Prod 74(1):91-100

Clark A III, Jordan L, Schimleck L, Daniels RF (2008) Effect of initial planting spacing on wood properties of unthinned loblolly pine at age 21. Forest Pro J 58(10):78-83

Cramer S, Kretschmann D, Lakes R, Schmidt T (2005) Earlywood and latewood elastic properties in loblolly pine. Holzforschung 59(5):531-538

Downie HF, Adu MO, Schmidt S, Otten W, Dupuy LX, White PJ, Valentine TA (2015) Challenges and opportunities for quantifying roots and rhizophere interactions through imaging and image analysis. Plant Cell Environ 38(7): 1213-1232

Faust TD, Clark A, Courchene CE, Shiver BD, Belli ML (1999) Effect of intensive forest management practices on wood properties and pulp yield of young, fast growing Southern pine. International Environmental Conference Preceding’s April 18-21, 1999, Nashville, Tenn (2):501-512

Fox TR, Jokela EJ, Allen HL (2007) The development of pine plantation silviculture in the southern United States. J Forest 105(7):337–347

Hartigan JA, and Wong MA (1979) A K-means clustering algorithm. Appl Stat 28(1):100-108

Hartley R, and Zisserman A (2003) Multiple view geometry in computer vision. Cambridge University Press.

Hijams RJ (2016) raster: Geographic data analysis and modeling. R package version 2.5-8. https://cran.r-project.org/web/packages/raster/raster.pdf

Howard J (2007) U.S. timber production, trade, consumption, and price statistics 1965 to 2005. USDA: Forest Products Laboratory. FPL-RP-637

Jokela EJ, Martin TA, Vogel JG (2009) Twenty-five years of intensive forest management with southern pines: important lessons learned. J Forest 108(7):338-347

Kanungo T, Netanyahu NS, Wu AY (2002) An efficient k-means clustering algorithm: analysis and implementation. IEEE T Pattern Anal 24(7):881-892

Lam F, Barret JD, Nakajima S (2003) Influence of knot area ratio on the bending strength of Canadian Douglas fir timber used in Japanese post and beam housing. J Wood Sci 51(1):18-25

Lam F, Barret JD, Nakajima S (2004) Influence of knot area ratio based grading rules on the engineering properties of Hem-fir used in Japanese post and beam housing. Wood Sci Technol 38(2):89-92

Madsen B (1992) Structural Behavior of Timber. 1st ed. North Vancouver, CAN: Timber Engineering. Print.

Mayer C, Windhager S, Schaefer K, Mitteroecker P (2017) BMI and WHR are reflected in female facial shape and texture: a geometric morphometric image analysis. PLOS ONE 12(2): 1-13

Oh JK, Shim K, Kim KM, Lee JJ (2009) Quantification of knots in dimension lumber using a single-pass X-ray radiation. J Wood Sci 55(4):264-272

Pebesma E, and Bivand R (2016) sp: Classes and methods for spatial data. R package version 1.2-4. https://cran.r-project.org/web/packages/sp/sp.pdf

Pfeffer MJ, Francis JD, Ross Z (2006) Farmland Change, Urbanization and a changing farm economy. Occasional Policy Brief Series

R Core Team (2017) R: a language and environment for statistical computing. R Foundation for Statistical Computing, Vienna, Austria. http://www.R-project.org/

Roblot G, Bléron L, Mériaudeau F, Marchal R (2010) Automatic computation of the knot area ratio for machine strength grading of Douglas-fir and Spruce timber. Eur J Environmental Civil Eng 14(10):1317-1332

Rossum GV (2007) Python Programming Language. USENIX Annual Technical Conference Vol. 41

RStudio (2017) RStudio: Integrated development environment for R (Version 3.3.1). Boston. Retrieved April 17, 2017

Russ JC, and Russ JC (2007) Introduction to image processing and analysis. Boca Raton, FL: Taylor & Francis. Print

Schajer GS (2001) Lumber strength grading using X-ray scanning. Forest Prod J 51(1):43-52

Schindelin J, Arganda-Carreras I, Frise E (2012) Fiji: an open-source platform for biological-image analysis. Nat Methods 9(7):676-682

Schultz RP (1999) Loblolly-the pine for the twenty-first century. New Forest 17:71-88

The GIMP team, GIMP 2.8.16, www.gimp.org, 1997-2017, retrieved on December, 2016

Vance ED, Maguire DA, Zalesney RS Jr (2010) Research strategies for increasing productivity of intensively managed forest plantations. J Forest 108:183–192

Wear DN, and Greis JG (2002) Southern forest resource assessment: Summary of findings. J Forest 100(7):6-14

Wickham H (2017) tidyr: Easily tidy data with ‘spread()’ and ‘gather’ functions. R package version 0.6.3. https://cran.r-project.org/web/packages/tidyr/tidyr.pdf

Zaborowicz M, Boniecki P, Koszela K, Przybylak A, Przybyl J (2017) Application of neural image analysis in evaluating the quality of greenhouse tomatoes. Sci Hortic-Amsterdam 218(2017): 222-229

CHAPTER 4: CONCLUSIONS

Due to the recent reduction in design values for visually graded southern pine design lumber, it is important to investigate the effects that knots have on lumber quality. Image analysis can be successfully used to quantify knots. This study showed that there was an inverse relationship between KAR and lumber stiffness and strength. Meaning, as the knottiness of the lumber increases, the lumber stiffness and strength decreases. A measure of knots ($KAR_{rectangle}$) can be used in conjunction with other measures of non-destructive evaluation of lumber to better predict lumber stiffness and strength. There was no difference in either knot quantification method based on model performance. Future knot analysis work can focus on improving image quality and by photographing all sides of the lumber. Improved image quality would significantly decrease image preparation time and possibly increase accuracy of the knot detection. In addition to that, better images could allow for wood grain deviation caused by knots, and potentially allow for 3D reconstruction of each piece of lumber and possible internal knot volume calculations.